Engineering Axial Intensity of Bessel Beams using Meta-axicons with Amplitude and Phase Control

Jerin Geogy George
Department of Electrical Engineering
Indian Institute of Technology Madras
Chennai, India
ee20d029@smail.iitm.ac.in

Shanti Bhattacharya
Department of Electrical Engineering
Indian Institute of Technology Madras
Chennai, India
shanti@ee.iitm.ac.in

***Abstract*—The paper presents a new method for generating Bessel beams with uniform axial intensity over a defined region by using metasurfaces. Bessel beams are well known for their non-diffracting nature, but their axial intensity varies considerably during propagation. To address this limitation, we propose using metasurfaces to control the amplitude and phase of the incident fields and thereby generate a uniform axial intensity Bessel beam. The unit cell used in this study is composed of coupled rectangular dielectric resonators with polysilicon as the dielectric material. Numerical simulations were conducted using COMSOL multiphysics to demonstrate the effectiveness of this approach.**

***Index Terms*—Bessel beam, metasurface, axial intensity**

I. INTRODUCTION

Bessel beams (BBs) are renowned for their propagation-invariant and self-healing properties [1][2]. These distinctive features are applicable in various fields such as imaging and laser material processing, where they can replace conventional Gaussian beams. However, reaching the full potential of these features is severely constrained due to the axial intensity variation of the BBs along the propagation direction. Different techniques have been proposed to manipulate the axial intensity of BBs [3][4][5][6]. One of these methods utilizes two diffractive optical elements. The first element shapes the incident field amplitude, which falls on the second element, imparting the required phase modulation [6]. Although this approach enables axial intensity engineering, it requires two elements, and since they are binary diffractive elements, the efficiency achieved is low.

Meta-optical elements refer to artificially engineered metasurfaces that enable precise control over the amplitude, phase, and polarization of an incident electromagnetic field. These optical elements are composed of nano-scatters and their lateral dimensions can be modified to spatially manipulate the incident field [7]. They are typically used to engineer the wavefront of the incident field to achieve the desired functionality of an equivalent refractive optical element. But the careful design of the scatterers enables these metasurfaces to manipulate the amplitude and phase of the incident field according to specific requirements.

In this paper, we present a numerical simulation for generating a uniform axial intensity Bessel beam using meta-axicons, within its depth of focus (DoF). The structure simulated can be fabricated using lithography techniques.

II. METHODOLOGY

An ideal Bessel beam has an infinite amount of energy and cannot be generated practically. However, a quasi-Bessel beam can be efficiently generated using an axicon. A plane wave incident on an axicon undergoes a transformation, forming multiple plane waves that propagate along the surface of a cone. In the near field of the axicon, the multiple plane waves interfere with each other, resulting in the formation of a Bessel pattern. The axial intensity observed in each z-plane after the axicon is a result of the interference of waves that have propagated from different radial sections of the axicon. Therefore, the axial intensity of the Bessel pattern can vary depending on the energy distribution in each radial section of the axicon. Figure 1 shows the variation in the axial intensity of a Bessel beam generated from an axicon with a plane wave input.

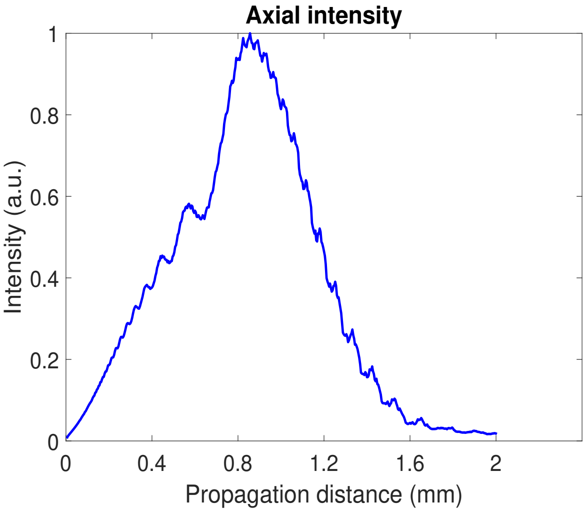

Fig. 1. Simulation of the axial intensity of a Bessel beam for plane wave illumination. The opening angle of the axicon used in 5^o and wavelength is 1550 nm

The axial intensity of the Bessel beam increases initially, attains its maximum value, and subsequently diminishes to negligible levels as the propagation distance reaches the depth of focus of the Bessel beam. The oscillatory nature of the axial intensity variation is a result of diffractive effects caused by the aperture of the axicon [2].

A. Uniform axial intensity Bessel beams

The axial intensity of a Bessel beam is directly proportional to the amount of energy present within a radial cross-section of the axicon and can be expressed as,

$$I_{ax} \propto I_{in}(r)2\pi r, \tag{1}$$

where $r = z\theta$. I_{in} is the input beam intensity, θ is the cone angle of the Bessel beam and z is the propagation distance. To achieve a uniform axial intensity distribution in a Bessel beam, amplitude modulation is required in addition to the conical wavefront imparted by an axicon. This can be done by illuminating the axicon with a desired beam intensity or by engineering the transmittance of the axicon. Traditional refractive and diffractive axicons are limited in their ability to incorporate spatially varying transmittance. However, the utilisation of metasurfaces enables the engineering of both transmittance and phase in axicons. For plane wave illumination, the transmittance of the meta-axicon should follow the below relation

$$T(r) \propto \frac{1}{r}, \tag{2}$$

to get uniform axial intensity. Here, T is the transmittance of the axicon. However, it is practically not possible to maintain a constant axial intensity from the z = 0 plane (immediately after the axicon). The amplitude modulation required to achieve this would result in an infinite energy requirement due to the infinitesimally small radius at the center of the beam.

In practice, a compromise is necessary, and a uniform axial intensity can be approximated by keeping the amplitude modulation constant in the central region of the beam. This allows the axial intensity to increase linearly initially and beyond a propagation distance the axial intensity will stabilize and remain constant. This approach can generate Bessel beams with reasonably uniform axial intensity over a finite propagation distance.

B. Design of meta-axicon

Conventional meta-optical elements designed for monochromatic applications typically rely on scatterers with cylindrical, rectangular, or fin-shaped geometries [8][9]. Although these structures perform well in terms of phase modulation, they lack the necessary flexibility to modulate both the amplitude and phase of the incident field simultaneously. Researchers have used more complex geometries like coupled rectangular resonators to realise multi-wavelength behaviour [10][11]. These structures contain two rectangular pillars in a single unit cell and the mutual coupling between the rectangular resonators provides an enhanced electromagnetic response with more design flexibility. This can be exploited to achieve simultaneous amplitude and phase modulation of the incident field. The unit cell structure of the coupled resonators is illustrated in fig. 2. In this paper, we have conducted only a 2D simulation due to computational limitations. Compared to a rectangular meta-atom, the coupled rectangular resonator structure offers more degrees of freedom, namely, the width of the resonators w1 and w2, as well as the gap between the resonators g.

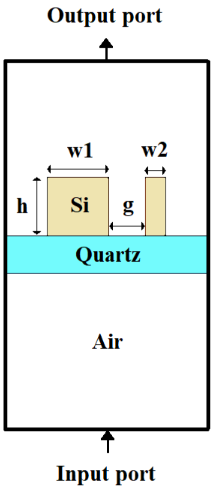

Fig. 2. Coupled rectangular resonators - metasurface unit cell.

The unit cell comprises dielectric rectangular resonators made of polysilicon on top of quartz. We have chosen a design wavelength of 1550 nm and a dielectric material with a high refractive index and low absorption coefficient at this wavelength. To generate a look-up map, we have conducted a unit cell simulation using the finite element method for determining the EM response by sweeping the design parameters over a range of values. The height of the pillars has been kept fixed (800 nm) to ensure a single lithography step. We used a periodic boundary condition while simulating the unit cells. However, it should be noted that this is an approximation as periodic boundary condition assumes an infinitely periodic structure. For ease of implementation, we have digitized the continuous transmittance and phase function into six target levels and determined suitable nanostructure geometries from the look-up map. The dimensions of the unit cells used for the simulation are given in Table 1. We then created the meta-optical element using different nanostructures and evaluated the near-field electromagnetic (EM) response. Using the Fresnel diffraction formula, we have evaluated the field at different propagation distances in the near field.

TABLE I
DETAILS OF UNIT CELLS USED FOR DESIGNING META-AXICONS

Uniform transmittance					**Hyperbolic transmittance**				
w1	w2	g	T	ϕ	w1	w2	g	T	ϕ
560	100	0	0.90	312	260	160	0	0.86	310
220	200	30	0.90	264	480	180	90	0.30	251
240	220	320	0.89	205	340	120	310	0.17	195
140	240	150	0.93	144	200	100	350	0.12	145
160	140	190	0.92	94	260	120	270	0.11	82
100	100	330	0.88	45	200	120	330	0.06	13

T is the transmittance; ϕ is the phase in degrees; w1, w2, and g are in nm; period of the unit cell is 850 nm and height of the unit cell is 800 nm

III. RESULTS AND DISCUSSIONS

We have designed two metasurfaces that provide axicon functionality. Figure 3 shows the near-field transmittance and phase after the metasurfaces simulated using 2D finite element method in COMSOL multiphysics. In the first design, the transmittance of the different resonators within the metasurface is nearly uniform, as shown in Figure 3A. In contrast, the transmittance in the second design decreases hyperbolically along the radial direction, as illustrated in Figure 3B. The radially decreasing transmittance is selected to ensure that the amplitude of the field immediately after the optical element varies inversely with the square root of the radial distance from the beam axis. Both of these designs alter the phase of an incoming field in a manner similar to that of an axicon. The fluctuations observed in both transmittance and phase (fig. 3A and fig. 3B) are attributed to mutual coupling between nearby unit cells.

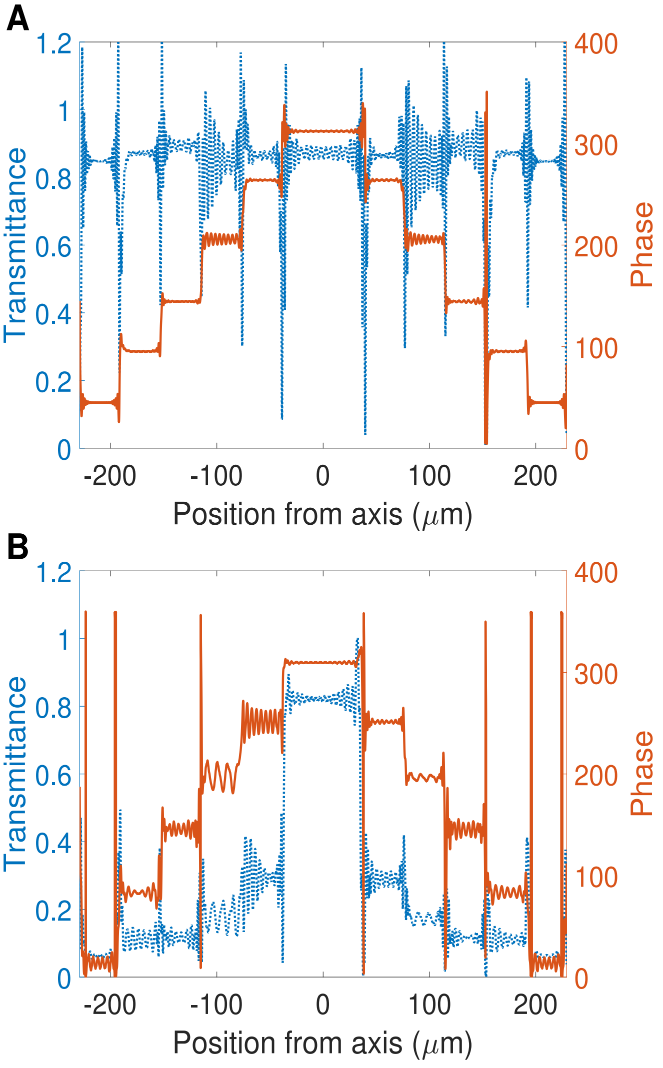

Fig. 3. 2D numerical simulation of meta-axicon. Near field transmittance and phase imparted by (A) first axicon - uniform transmittance, and (B) second axicon - hyperbolic transmittance

Figure 4 shows the Bessel beam profiles generated at a propagation distance of 16 mm using two different meta-axicon designs. The first design incorporates resonators with uniform transmittance, resulting in significantly higher axial intensity compared to the second design, which has a hyperbolic decrease in transmittance radially. This reduction in axial intensity in the second design can be attributed to the lower transmittance of the nanostructures.

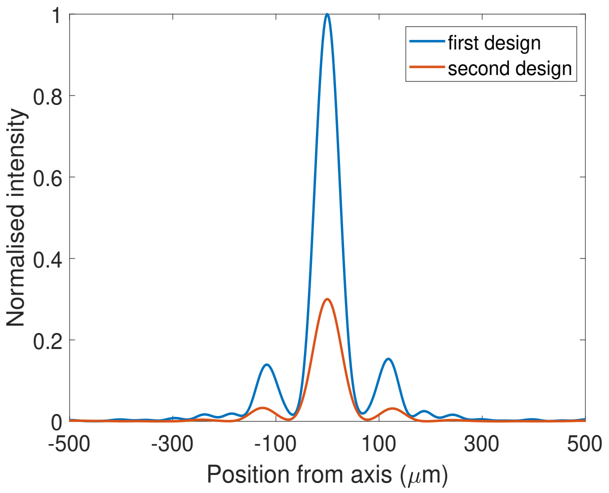

Fig. 4. Bessel beam profile at a propagation distance of 16 mm. first design - uniform transmittance meta-axicon, second design - hyperbolic transmittance meta-axicon

Figure 5 shows the change in axial intensity along the direction of propagation for the two metasurfaces. The first metasurface has resonators with nearly uniform transmittance, resulting in an increase in axial intensity with increasing propagation distance. However, as the propagation distance approaches the depth of focus of the axicon, the axial intensity begins to decrease. In contrast, the second metasurface utilizes resonators with a hyperbolic variation in transmittance. As a result, the axial intensity remains relatively uniform for a certain propagation distance, after which it starts to decrease. The oscillation in the axial intensity variation and the drop in the axial intensity near the depth of focus are due to diffraction. Beyond the depth of focus, the Bessel beam starts to diverge and the axial intensity decreases rapidly.

The designed metasurfaces can be fabricated using electron beam lithography and associated pattern transfer techniques. Initially, the dielectric material (poly-Si) for the required thickness (800 nm) can be deposited on a quartz substrate using low-pressure chemical vapour deposition or plasma-enhanced chemical vapour deposition. Then an e-beam resist can be coated on top of this layer and patterned using e-beam exposure. After developing the resist, a metallisation process using e-beam evaporation or thermal evaporation followed by lift-off can be done for making a hard mask to etch the dielectric layer. Typically, inductively coupled plasma reactive ion etching (ICPRIE) is used to etch the dielectric layer. ICPRIE is a dry etching technique which gives good vertical

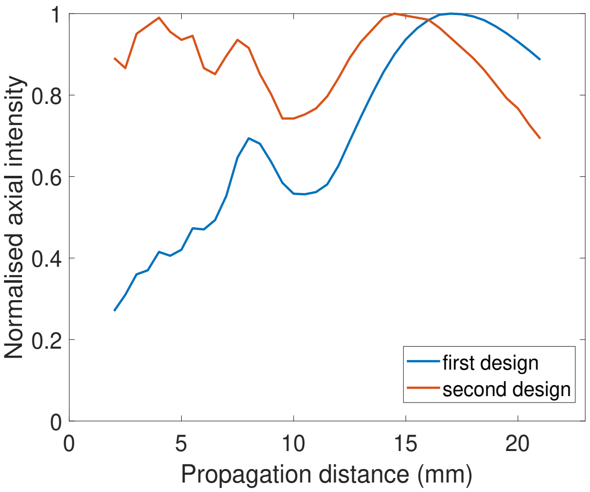

Fig. 5. Axial intensity variation. first design - increasing axial intensity with uniform transmittance, second design - uniform axial intensity with hyperbolic transmittance

sidewalls after etching. Finally, the metal mask can be removed by etching and the device can be optically characterised to analyse the performance.

In our numerical simulation, we considered a 2D model to reduce computational costs. This approximation assumes that one dimension is significantly larger than the other, allowing us to reduce the complexity of the simulation. While it is possible to fabricate such structures with advanced lithography techniques, it presents challenges when it comes to etching narrow gaps between elongated ridges. Alternatively, a similar approach can be followed to design a 3D model. This would introduce two additional design parameters associated with the length of the resonators. In this case, the metasurface would comprise nanostructures resembling rectangular pillars. Fabricating these pillar-like structures is generally less challenging than creating ridge-like structures resulting from the current 2D design. However, it is important to note that fully simulating the 3D model would require significantly higher computational memory.

CONCLUSION

We have presented a method using metasurfaces to engineer the axial intensity of Bessel beams. We also designed and demonstrated a uniform axial intensity Bessel beam through 2D numerical simulation. The axial intensity can be engineered by properly tuning the transmittance and phase of the metasurface. The metasurface design can be converted to 3D and can be fabricated with lithography techniques.

ACKNOWLEDGMENT

The authors acknowledge financial support from the Ministry of Human Resource Development, New Delhi through the SPARC project (Sanction No. SPARC/2018-2019/P796/SL).

REFERENCES

[1] J. Durnin, J. Miceli Jr, and J. H. Eberly, “Diffraction-free beams,” *Physical review letters*, vol. 58, no. 15, p. 1499, 1987.
[2] D. McGloin and K. Dholakia, “Bessel beams: Diffraction in a new light,” *Contemporary physics*, vol. 46, no. 1, pp. 15–28, 2005.
[3] Z. Jaroszewicz, J. Sochacki, A. Kołodziejczyk, and L. R. Staronski, “Apodized annular-aperture logarithmic axicon: Smoothness and uniformity of intensity distributions,” *Optics letters*, vol. 18, no. 22, pp. 1893–1895, 1993.
[4] M. Zamboni-Rached, “Stationary optical wave fields with arbitrary longitudinal shape by superposing equal frequency bessel beams: Frozen waves,” *Optics Express*, vol. 12, no. 17, pp. 4001–4006, 2004.
[5] T. Čižmár and K. Dholakia, “Tunable bessel light modes: Engineering the axial propagation,” *Optics express*, vol. 17, no. 18, pp. 15 558–15 570, 2009.
[6] R. Dharmavarapu, S. Bhattacharya, and S. Juodkazis, “Diffractive optics for axial intensity shaping of bessel beams,” *Journal of Optics*, vol. 20, no. 8, p. 085 606, 2018.
[7] Q. Zhao, J. Zhou, F. Zhang, and D. Lippens, “Mie resonance-based dielectric metamaterials,” *Materials today*, vol. 12, no. 12, pp. 60–69, 2009.
[8] M. Decker, I. Staude, M. Falkner, *et al.*, “High-efficiency dielectric huygens’ surfaces,” *Advanced Optical Materials*, vol. 3, no. 6, pp. 813–820, 2015.
[9] R. Dharmavarapu, K.-i. Izumi, I. Katayama, *et al.*, “Dielectric cross-shaped-resonator-based metasurface for vortex beam generation at mid-ir and thz wavelengths,” *Nanophotonics*, vol. 8, no. 7, pp. 1263–1270, 2019.
[10] F. Aieta, M. A. Kats, P. Genevet, and F. Capasso, “Multiwavelength achromatic metasurfaces by dispersive phase compensation,” *Science*, vol. 347, no. 6228, pp. 1342–1345, 2015.
[11] J. G. George, S. Thomas, and S. Bhattacharya, “Design of multi-wavelength dielectric metasurfaces using finite element software,” *Asian Journal of Physics*, vol. 30, no. 4, pp. 623–632, 2021.